

Direct visualization of the thermomagnetic behavior of pseudo–single-domain magnetite particles

Trevor P. Almeida,^{1*} Adrian R. Muxworthy,¹ András Kovács,² Wyn Williams,³ Paul D. Brown,⁴ Rafal E. Dunin-Borkowski²

2016 © The Authors, some rights reserved; exclusive licensee American Association for the Advancement of Science. Distributed under a Creative Commons Attribution License 4.0 (CC BY). 10.1126/sciadv.1501801

The study of the paleomagnetic signal recorded by rocks allows scientists to understand Earth's past magnetic field and the formation of the geodynamo. The magnetic recording fidelity of this signal is dependent on the magnetic domain state it adopts. The most prevalent example found in nature is the pseudo–single-domain (PSD) structure, yet its recording fidelity is poorly understood. Here, the thermoremanent behavior of PSD magnetite (Fe_3O_4) particles, which dominate the magnetic signatures of many rock lithologies, is investigated using electron holography. This study provides spatially resolved magnetic information from individual Fe_3O_4 grains as a function of temperature, which has been previously inaccessible. A small exemplar Fe_3O_4 grain (~150 nm) exhibits dynamic movement of its magnetic vortex structure above 400°C, recovering its original state upon cooling, whereas a larger exemplar Fe_3O_4 grain (~250 nm) is shown to retain its vortex state on heating to 550°C, close to the Curie temperature of 580°C. Hence, we demonstrate that Fe_3O_4 grains containing vortex structures are indeed reliable recorders of paleodirectional and paleointensity information, and the presence of PSD magnetic signals does not preclude the successful recovery of paleomagnetic signals.

INTRODUCTION

Magnetic minerals in rocks record the signal from Earth's magnetic field at the time of their formation, providing key information on past geomagnetic field behavior and tectonic plate motion (1). In the field of paleomagnetism, understanding the stability of recorded magnetizations over geological time scales is critical for the recovery of meaningful intensity and directional information (2). The grain size of magnetic recorders has a significant influence on the stability of the acquired signal because of the capacity of a grain's volume to energetically favor certain magnetic domain structures (3). It has long been known that small, magnetically near-uniform, single-domain (SD) grains (typically <80 nm for magnetite) retain the most reliable magnetic signals over long time periods (4). However, the magnetic signature in most rocks is usually dominated by larger magnetic grains (~0.1 to 10 μm) that display nonuniform magnetic structures (that is, vortices, etc.), commonly referred to as pseudo-SD (PSD) particles because their bulk magnetic characteristics are similar, but not identical, to SD particles.

In igneous rocks, the main magnetic recording mechanism is termed thermoremanent magnetization (TRM) (5), which is acquired in the direction of the ambient geomagnetic field as grains cool below their Curie temperature (T_C ~ 580°C for magnetite). Current understanding of the thermomagnetic behavior of PSD remanence is informed by bulk magnetic measurements and numerical models (6–8), but the latter still require much improvement to elucidate the intricate details of PSD sta-

bility and transition states with temperature. Consequently, our knowledge of PSD remanence as a function of temperature is poor, and our understanding of magnetic stability and, hence, the reliability of most planetary paleomagnetic signals is limited.

The direct visualization of PSD magnetic structures during in situ heating close to their T_C has the potential to revolutionize our knowledge of the behavior and stability of recorded paleomagnetic signals. Acquiring such experimental measurements provides a new level of detail because the lowest-energy magnetic configurations predicted from micromagnetic simulations are often not observed experimentally, information about the specimen is rarely known with high enough precision to accurately describe the specimen in simulations, and magnetic states are not always reproducible. In this context, we apply the transmission electron microscopy (TEM) technique of off-axis electron holography, the only technique that can provide high-resolution images of magnetic domain states in nanometric grains (9–12), to the study of PSD magnetite (Fe_3O_4) remanence during in situ heating. The magnetic behaviors of ~20 Fe_3O_4 PSD powder grains were examined as a function of temperature up to 550°C, just below their T_C , to understand their different magnetic responses as a function of particle size. The two exemplar PSD grains presented in this study satisfied the requisite conditions of individual isolation and magnetic response in a PSD state while remaining physically stable during in situ heating.

RESULTS

The thermomagnetic behavior of a small PSD Fe_3O_4 grain (fig. S1), heated from 20° to 550°C and then cooled back to 20°C, is shown in Fig. 1. The bright-field TEM image of Fig. 1A shows the Fe_3O_4 grain (labeled G1) to exhibit an almost rhombus shape in two-dimensional (2D) projection and be ~150 nm in length across its long-diagonal axis. Figure 1B presents a magnetic induction map of the Fe_3O_4 grain, constructed

¹Department of Earth Science and Engineering, Imperial College London, South Kensington Campus, London SW7 2AZ, UK. ²Ernst Ruska–Centre for Microscopy and Spectroscopy with Electrons and Peter Grünberg Institute, Forschungszentrum Jülich, D-52425 Jülich, Germany. ³School of GeoSciences, University of Edinburgh, The King's Buildings, West Mains Road, Edinburgh EH9 3JW, UK. ⁴Department of Mechanical, Materials and Manufacturing Engineering, Faculty of Engineering, University of Nottingham, University Park, Nottingham NG7 2RD, UK.

*Corresponding author: E-mail: trevor.almeida@glasgow.ac.uk

†Present address: School of Physics and Astronomy, Kelvin Building, University of Glasgow, Glasgow G12 8QQ, UK.

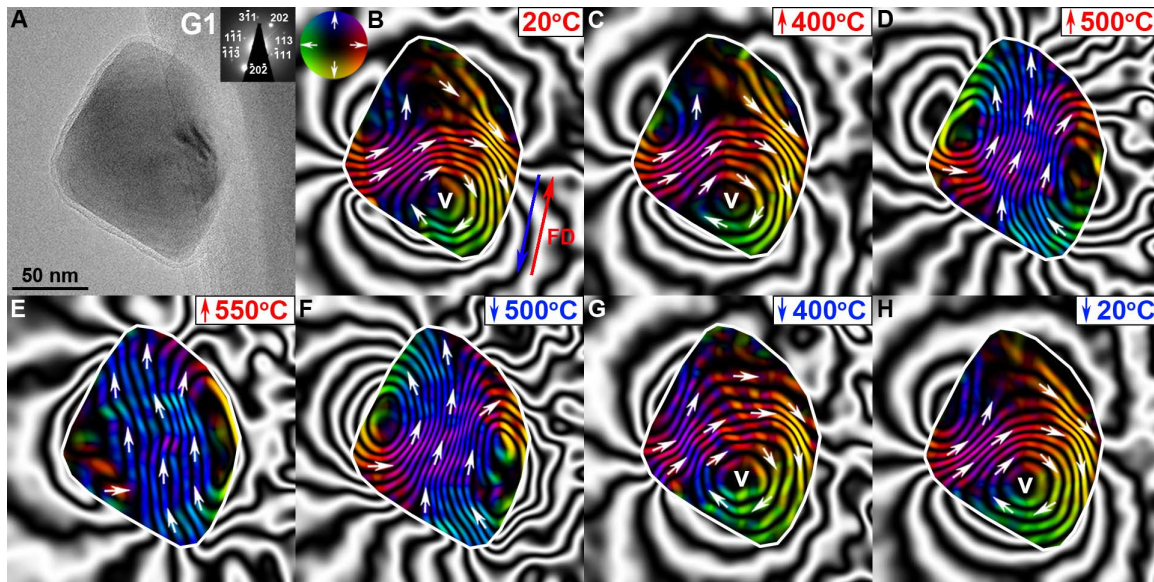


Fig. 1. Visualization of the thermomagnetic behavior of a small PSD Fe_3O_4 grain (sample G1). (A) Bright-field TEM image of the individual Fe_3O_4 grain (~150 nm in length across its long-diagonal axis), with associated electron diffraction pattern inset. (B to H) Magnetic induction maps reconstructed from holograms taken at (B) 20°C (with the red arrow, labeled FD, showing the direction of the in-plane component of the applied saturating field to induce magnetic remanence, whereas the blue arrow shows the additional direction the field was applied for the calculation of the mean inner potential); during in situ heating to (C) 400°C, (D) 500°C, and (E) 550°C; upon subsequent cooling to (F) 500°C, (G) 400°C, and (H) 20°C. The contour spacing is 0.098 rad for all the magnetic induction maps, and the magnetization direction is shown using arrows, as depicted in the color wheel. v, center of the vortex.

from electron holograms (fig. S3) acquired at room temperature (20°C) after being initially magnetized using a saturating field, and reveals its magnetization to flow generally from left to right along the short-diagonal axis and to interact with a small vortex core (denoted v), along with a component of stray magnetic field, which is characteristic of a PSD state. The associated magnetic induction map of Fig. 1C, acquired at 400°C, shows the Fe_3O_4 grain to display a very similar magnetization as the grain at room temperature (Fig. 1B), that is, the strength and direction of the magnetization are essentially unchanged and stable with heating from 20° to 400°C (fig. S4, A to C). However, the remanent PSD state changes markedly when the temperature increases to 500°C (Fig. 1D), with the magnetic contours narrowing and aligning along the long-diagonal axis and curving away from this axis at the top and bottom of the grain. The magnetic contour density of the vortex structures at $\leq 400^\circ\text{C}$ (where the magnetic intensity would be the largest) is less than the contour density at 500°C; hence, it is considered that a large component of the magnetization in Fig. 1B is oriented out-of-plane (fig. S5, A and B), which then rotates to lie in-plane at 500°C. A further increase in temperature to 550°C (Fig. 1E) induces a widening of the magnetic contours that become more closely aligned with the long-diagonal axis. These magnetic states at 500° and 550°C could be misinterpreted as SD; however, because the flux loops on either side of the central magnetic contours are contained within the Fe_3O_4 grain, they are more likely to be vortex states that are observed edge-on (fig. S5, C to F) (13, 14). On cooling to 500°C, the magnetic induction map (Fig. 1F) resorts back to the state seen in Fig. 1D, and a further decrease in temperature to 400°C (Fig. 1G) recovers the original PSD state, similar to that shown in Fig. 1C, albeit with slightly wider contours spread further along the short-diagonal axis. Upon cooling to 20°C (fig. S4, D to F), the magnetic arrangement (Fig. 1H) is very similar to its initial state before heating, with the contours flowing from left to right along

the short-diagonal axis, and interacting again with a small vortex core (located toward the bottom of the grain), along with a component of stray magnetic field. A thin (<5 nm) layer of amorphous carbon on the grain surface (Fig. 1A), considered a by-product from the initial heating of the grain on the carbon film, is suggested to have a beneficial effect of protecting the grain from oxidization during multiple heating.

The second thermomagnetic sequence presented (Fig. 2 and fig. S6, A to F) illustrates the magnetization of a slightly larger Fe_3O_4 grain (labeled G2), also rhombus-shaped in 2D projection and ~250 nm in length across its long-diagonal axis (Fig. 2A). In this case, the room temperature magnetization resides in a vortex state (denoted v), again characteristic of a PSD state. An increase in temperature to 400°C leads to a widening of the magnetic contours (Fig. 2C), the intensity decreases further at 500°C (Fig. 2D), and a significantly weakened magnetization remains at 550°C, although the vortex state is retained (Fig. 2E). The magnetic intensity then increases upon cooling back to 500° and 400°C (Fig. 2, F and G, respectively), with its room temperature state (Fig. 2H) being similar to that of its original state (Fig. 2B).

DISCUSSION

This in situ TEM, off-axis electron holography investigation has provided fundamental insight into the effects of temperature on the remanent magnetization of individual Fe_3O_4 PSD grains. The two exemplar grains presented display PSD magnetization domain structures at room temperature but exhibit particularly different thermomagnetic behaviors with heating close to their T_C of ~580°C (12, 15), and it is evident that grain size plays an important role in their thermomagnetic response.

The smaller grain (G1; Fig. 1) maintains a stable PSD state up to 400°C but transforms markedly upon heating to 500° and 550°C.

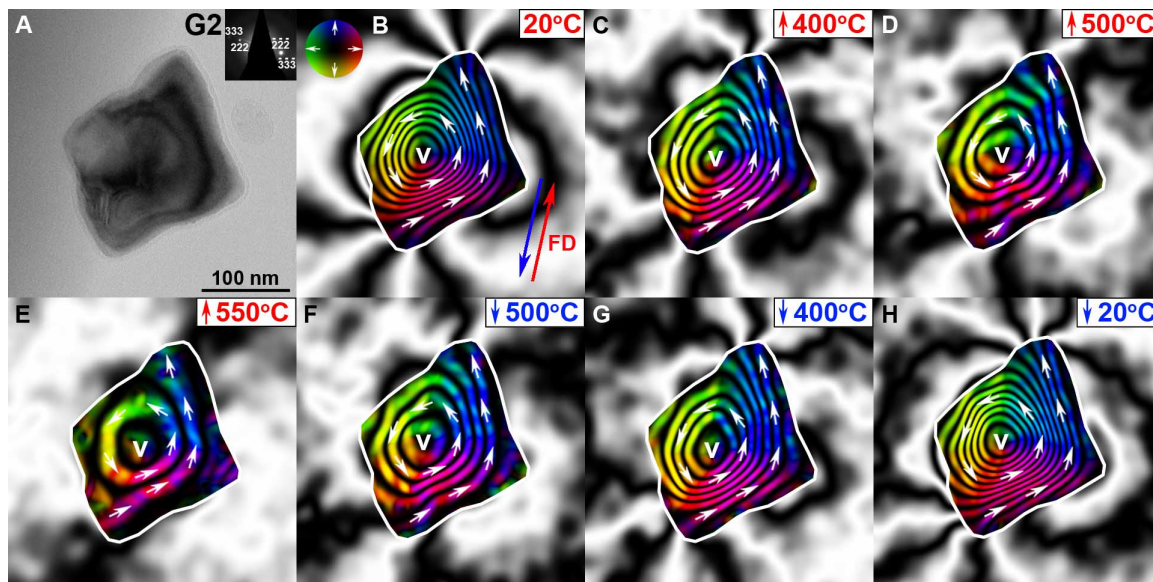


Fig. 2. Visualization of the thermomagnetic behavior of a slightly larger PSD Fe_3O_4 grain (sample G2). (A) Bright-field TEM image of an individual Fe_3O_4 grain (~ 250 nm in length across its long-diagonal axis), with associated electron diffraction pattern inset. (B to H) Magnetic induction maps reconstructed from holograms taken at (B) 20°C (with the red arrow, labeled FD, showing the direction of the in-plane component of the applied saturating field to induce magnetic remanence, whereas the blue arrow shows the additional direction the field was applied for the calculation of the mean inner potential); during in situ heating to (C) 400°C , (D) 500°C , and (E) 550°C ; upon subsequent cooling to (F) 500°C , (G) 400°C , and (H) 20°C . The contour spacing is 0.53 rad for all the magnetic induction maps, and the magnetization direction is shown using arrows, as depicted in the color wheel.

Figure 1D shows that flux loops on either side of central magnetic contours are contained within the Fe_3O_4 grain, indicative of a vortex state observed edge-on (13, 14). Hence, it is interpreted that the vortex core rotates and aligns with the long-diagonal axis of the Fe_3O_4 grain during heating. This is consistent with the high-temperature behavior predicted by micromagnetic models of similarly sized (~ 120 nm) Fe_3O_4 cubes, where energy barriers associated with the transitions between two vortex states are readily overcome at elevated temperature (6). Further heating to 550°C induces a strict alignment of the vortex core, parallel to the long-diagonal axis, attributed to a combination of shape anisotropy and a reduction of the vorticity of this PSD state. The reduced vorticity is due to a decrease in spontaneous magnetization with increasing temperature, as evidenced by widening of the magnetic contours. Upon cooling, the PSD state seen before heating is recovered, confirming that this original PSD arrangement is the favored lower-energy state at room temperature. The larger grain (G2; Fig. 2) exhibits a more thermomagnetically stable PSD state, with retention of its vortex state and stray magnetic field up to 550°C , while only showing a decrease in magnetic intensity, which is then recovered upon cooling. This enhanced thermomagnetic stability is attributed to the larger volume of this grain, which exhibits inherently higher energy barriers between possible PSD states; this vortex structure is the preferred state at temperatures closer to T_C of $\sim 580^\circ\text{C}$.

It is evident that grain size has little influence on remanent magnetic signals below $\sim 400^\circ\text{C}$, with only the intensity of the domain structures being affected, and PSD grains are generally considered to retain their directional information below this temperature, with reduction in intensity being simply associated with a drop in spontaneous magnetization. However, above $\sim 400^\circ\text{C}$, the stability of the directional information associated with remanence is variable, with the PSD grain size playing a critical role in the fidelity of the remanent magnetic signal.

The “unblocking” of a stable state and subsequent transition to a lower-energy domain structure at elevated temperature depends on competing magnetic energies that are strongly dependent on grain volume and shape. The magnetization of the vortex structure in the larger PSD grain (G2) is more stable at high temperatures than that of the smaller PSD grain (G1), the key point being that smaller PSD grains unblock and transition at lower temperatures. SD grains are considered the most reliable magnetic recorders, and as their grain size increases, they unblock at higher temperatures approaching T_C . However, once a critical size is reached where a vortex state, that is, a PSD state, becomes favorable at room temperature (~ 100 nm for magnetite) (16, 17), this study shows that the unblocking temperature decreases sharply to between $\sim 400^\circ$ and 500°C , then gradually increases again as the PSD grain size increases further. Hence, if we increased the grain size from a stable SD state between $\sim 400^\circ$ and 500°C , we would expect the following transition: stable SD \rightarrow dynamic vortex \rightarrow stable vortex. Most importantly, the directional information is recovered upon cooling to 400°C , despite the instability of domain structures as observed at temperatures $>400^\circ\text{C}$ in grains close to the SD to PSD transition size range (~ 100 to 200 nm). Hence, this study has demonstrated that smaller PSD grains, previously considered nonideal recorders, recover both their directional and intensity information after heating close to the T_C . Indeed, magnetic domain states exist in three dimensions, and the change in strength and direction of the magnetization within the Fe_3O_4 grains during heating suggests a greater degree of complexity than can be fully accessed by 2D in-plane representations of magnetization. Improvement of 3D micromagnetic models to accurately incorporate thermal effects and comparison of their produced simulated magnetic induction maps with experimental results could elucidate the 3D nature of the transformations observed in these magnetic domain states in the future, providing fundamental insight into the effect of temperature on magnetic recording fidelity.

It is clear that grain size has a critical influence on the stability of recorded paleomagnetic signals in samples with evidence of heating (for example, thermal overprints), and there has long been ambiguity regarding the reliability of the magnetic signal acquired by grains in the PSD size range, cited as wide as ~ 0.1 to $10\ \mu\text{m}$ for magnetite (2). One recent study of samples containing Ti-rich magnetite grains, ~ 2 to $20\ \mu\text{m}$ in diameter, proposed that PSD TRM and multidomain (MD) TRM, that is, larger grains with many domain structures, are unreliable recorders of intensity (18) because of the relaxation of closure domain walls on time scales of ~ 1 year. In contrast, the sizes of pure magnetite PSD grains studied here are an order-of-magnitude smaller ($\leq 250\ \text{nm}$ in diameter) and represent what we consider to be true PSD behavior, that is, vortex structures without closure domain walls that are seen only for particles $> 1\ \mu\text{m}$ in micromagnetic models (19). In summary, PSD vortex structures behave like stable uniaxial SD particles, with high blocking/unblocking temperatures that are unlikely to display viscosity, making them excellent paleomagnetic recorders.

When more than millions of PSD vortex carriers (~ 100 to $1000\ \text{nm}$), as commonly found in bulk paleomagnetic samples, are averaged, there will be net partial alignment of the grains' magnetic moments with the ambient field during TRM acquisition, yielding a small net magnetization, in a similar fashion to assemblages of SD grains. Similarly, there will be a range of unblocking volumes, although the relationship with unblocking temperature will not be monotonic for SD grains. The high unblocking temperature of PSD vortex structures means that their TRM will be metastable on geological time scales, that is, $> 5\ \text{Ga}$ (20). Hence, whereas MD TRM may be considered unreliable, we have demonstrated that "true" PSD TRM, that is, vortex states that are ubiquitous in rocks and meteorites (15, 21), is indeed a reliable recorder of paleodirectional and paleointensity information.

MATERIALS AND METHODS

Sample details

A powder of hydrothermally synthesized Fe_3O_4 particles, with sizes ranging from ~ 150 to $\sim 250\ \text{nm}$, was purchased from Nanostructured and Amorphous Materials. For the purpose of in situ heating TEM investigations, the Fe_3O_4 powder was dispersed in ethanol using an ultrasonic bath before deposition onto an EMheaterchip, with silicon nitride (SiN) membranes and small windows of either carbon or SiN film, which was then inserted into a single-tilt TEM sample heating holder (DENSsolutions).

In situ TEM and magnetic imaging

Off-axis electron holograms were acquired at $300\ \text{kV}$ in Lorentz mode in a Titan 80-300 TEM with a charge-coupled device camera and an electron biprism operated typically at $90\ \text{V}$ (Ernst Ruska-Centre for Microscopy and Spectroscopy with Electrons, Forschungszentrum Jülich, Germany). The samples were preheated to 700°C in the TEM in situ for the purpose of evaporating remaining water and to alleviate any possible strain induced during particle synthesis. The directions of magnetization in the Fe_3O_4 particles were reversed initially at room temperature in situ in the TEM by tilting the sample by $\pm 75^\circ$ and turning on the conventional microscope objective lens to apply a magnetic field of $> 1.5\ \text{T}$ to the sample, parallel to the direction of the electron beam. The objective lens was then turned off, and the sample was tilted back to 0° for hologram acquisition under field-free

conditions (residual field $< 0.2\ \text{mT}$) with the particles induced with a room temperature saturation isothermal remanent magnetization (SIRM). Holograms were recorded for each particle magnetized in opposite directions, and the mean inner potential (MIP) was separated from the magnetic potential, as described by Dunin-Borkowski *et al.* (9). Electron holograms were then acquired under field-free conditions during in situ heating at 100°C intervals from 100° up to 500°C , then at 50°C interval up to 550°C , and again upon cooling, with each acquisition time being $8\ \text{s}$. Heating and cooling were performed at a rate of $50^\circ\text{C}/\text{min}$ using a single-tilt DENSsolutions heating holder, with the temperature displayed on the DENSsolutions temperature control. A temporary magnetic field of $< 50\ \mu\text{T}$ was estimated to be generated by the DENSsolutions holder during the in situ heating of the samples. Each heating experiment was then repeated, and magnetization reversal was performed by turning on the objective lens at $\pm 75^\circ$ at each temperature interval to obtain the MIP. The MIP was subtracted from the unwrapped total phase shift, acquired at each temperature interval during the initial heating experiment, to allow for the construction of magnetic induction maps representative of the magnetic remanence. For construction of the magnetic induction maps, the cosine of the magnetic contribution to the phase shift was amplified to produce magnetic phase contours. Colors were added to the contours to show the direction of the projected induction, as denoted by the color wheels.

SUPPLEMENTARY MATERIALS

Supplementary material for this article is available at <http://advances.sciencemag.org/cgi/content/full/2/4/e1501801/DC1>

X-ray diffractometry

In situ heating within the TEM

Off-axis electron holography

fig. S1. X-ray diffraction pattern of the Fe_3O_4 powder.

fig. S2. Images of DENSsolutions Wildfire in situ heating holder and EMheaterchips.

fig. S3. Schematic diagram of the setup for off-axis electron holography.

fig. S4. Magnetic induction maps of sample G1 at intermediate stages of heating and cooling.

fig. S5. Magnetic induction maps and proposed 3D forms of vortex states in sample G1.

fig. S6. Magnetic induction maps of sample G2 at intermediate stages of heating and cooling.

fig. S7. Magnetic induction maps and proposed 3D forms of vortex states in sample G2.

REFERENCES AND NOTES

1. R. T. Merrill, M. W. McElhinny, P. L. McFadden, *The Magnetic Field of the Earth: Paleomagnetism, the Core and the Deep Mantle* (Academic Press, London, 1996), pp. 531.
2. D. J. Dunlop, Ö. Özdemir, *Rock Magnetism: Fundamentals and Frontiers* (Cambridge Univ. Press, New York, 2001), pp. 577.
3. D. J. Dunlop, K. S. Argyle, Separating multidomain and single-domain-like remanences in pseudo-single-domain magnetites (215–540 nm) by low-temperature demagnetisation. *J. Geophys. Res.* **96**, 2007–2017 (1991).
4. L. Néel, Some theoretical aspects of rock-magnetism. *Adv. Phys.* **4**, 191–243 (1955).
5. D. J. Dunlop, Thermoremanent magnetization in submicroscopic magnetite. *J. Geophys. Res.* **78**, 7602–7613 (1973).
6. A. R. Muxworthy, D. J. Dunlop, W. Williams, High-temperature magnetic stability of small magnetite particles. *J. Geophys. Res.* **108**, 2281 (2003).
7. L. C. Thomson, R. J. Enkin, W. Williams, Simulated annealing of three-dimensional micromagnetic structures and simulated thermoremanent magnetization. *J. Geophys. Res.* **99**, 603–609 (1994).
8. M. Winklhofer, K. Fabian, F. Heider, Magnetic blocking temperatures of magnetite calculated with a three-dimensional micromagnetic model. *J. Geophys. Res.* **102**, 22695–22709 (1997).
9. R. E. Dunin-Borkowski, M. R. McCartney, R. B. Frankel, D. A. Bazylinski, P. R. Buseck, Magnetic microstructure of magnetotactic bacteria by electron holography. *Science* **282**, 1868–1870 (1998).
10. R. J. Harrison, R. E. Dunin-Borkowski, A. Putnis, Direct imaging of nanoscale magnetic interactions in minerals. *Proc. Nat. Am. Soc. U.S.A.* **99**, 16556–16561 (2002).
11. T. P. Almeida, T. Kasama, A. R. Muxworthy, W. Williams, L. Nagy, T. W. Hansen, P. D. Brown, R. E. Dunin-Borkowski, Visualised effect of oxidation on magnetic recording fidelity in pseudo-single-domain magnetite particles. *Nat. Comm.* **5**, 5154 (2014).

12. T. P. Almeida, T. Kasama, A. R. Muxworthy, W. Williams, L. Nagy, R. E. Dunin-Borkowski, Observing thermomagnetic stability of nonideal magnetite particles: Good palaeomagnetic recorders? *Geophys. Res. Lett.* **41**, 7041–7047 (2014).
13. M. J. Hÿtch, R. E. Dunin-Borkowski, M. R. Scheinfein, J. Moulin, C. Duhamel, F. Mazaleyrat, Y. Champion, Vortex flux channeling in magnetic nanoparticle chains. *Phys. Rev. Lett.* **91**, 257207 (2003).
14. R. K. K. Chong, R. E. Dunin-Borkowski, T. Kasama, M. J. Hÿtch, M. R. McCartney, Off-axis electron holography and image spectroscopy of ferromagnetic FeNi nanoparticles. *Inst. Phys. Conf. Ser.* **179**, 451–454 (2004).
15. T. P. Almeida, A. R. Muxworthy, W. Williams, T. Kasama, R. E. Dunin-Borkowski, Magnetic characterization of synthetic titanomagnetites: Quantifying the recording fidelity of ideal synthetic analogs. *Geochem. Geophys. Geosyst.* **15**, 161–175 (2014).
16. A. R. Muxworthy, W. Williams, Critical single-domain/multidomain grain sizes in noninteracting and interacting elongated magnetite particles: Implications for magnetosomes. *J. Geophys. Res.* **111**, 1–7 (2006).
17. W. Williams, D. J. Dunlop, Three-dimensional micromagnetic modelling of ferromagnetic domain structure. *Nature* **337**, 634–637 (1989).
18. L. V. de Groot, K. Fabian, I. A. Bakelaar, M. J. Dekkers, Magnetic force microscopy reveals meta-stable magnetic domain states that prevent reliable absolute palaeointensity experiments. *Nat. Comm.* **5**, 4548 (2014).
19. L. Nagy, thesis, University of Edinburgh (2015).
20. J. A. Tarduno, R. D. Cottrell, W. J. Davis, F. Nimmo, R. K. Bono, A Hadean to Paleoproterozoic geodynamo recorded by single zircon crystals. *Science* **349**, 521–524 (2015).
21. R. R. Fu, B. P. Weiss, E. A. Lima, R. J. Harrison, X.-N. Bai, S. J. Desch, D. S. Ebel, C. Suavet, H. Wang, D. Glenn, D. Le Sage, T. Kasama, R. L. Walsworth, A. T. Kuan, Solar nebula magnetic fields recorded in the Semarkona meteorite. *Science* **346**, 1089–1092 (2014).

Acknowledgments: We would like to thank the Ernst Ruska–Centre for Microscopy and Spectroscopy with Electrons at Forschungszentrum Jülich for use of their microscopy facilities. **Funding:** This work was funded by the Natural Environment Research Council (grant NE/J020966/1) and the European Research Council (advanced grant 320832). **Author contributions:** T.P.A. designed and carried out the experiments; A.R.M., W.W., and R.E.D.-B. conceived the study and supervised the research; A.K. assisted with the experimental work and analysis; T.P.A. led the writing of the paper with contributions from A.R.M., P.D.B., A.K., and R.E.D.-B. **Competing interests:** The authors declare that they have no competing interests. **Data and materials availability:** All data needed to evaluate the conclusions of this study are present in the paper and/or the Supplementary Materials. Additional data related to this paper may be requested from the authors.

Submitted 10 December 2015

Accepted 23 March 2016

Published 15 April 2016

10.1126/sciadv.1501801

Citation: T. P. Almeida, A. R. Muxworthy, A. Kovács, W. Williams, P. D. Brown, R. E. Dunin-Borkowski, Direct visualization of the thermomagnetic behavior of pseudo-single-domain magnetite particles. *Sci. Adv.* **2**, e1501801 (2016).

This article is published under a Creative Commons license. The specific license under which this article is published is noted on the first page.

For articles published under [CC BY](#) licenses, you may freely distribute, adapt, or reuse the article, including for commercial purposes, provided you give proper attribution.

For articles published under [CC BY-NC](#) licenses, you may distribute, adapt, or reuse the article for non-commercial purposes. Commercial use requires prior permission from the American Association for the Advancement of Science (AAAS). You may request permission by clicking [here](#).

***The following resources related to this article are available online at
<http://advances.sciencemag.org>. (This information is current as of January 31, 2017):***

Updated information and services, including high-resolution figures, can be found in the online version of this article at:

<http://advances.sciencemag.org/content/2/4/e1501801.full>

Supporting Online Material can be found at:

<http://advances.sciencemag.org/content/suppl/2016/04/11/2.4.e1501801.DC1>

This article **cites 18 articles**, 3 of which you can access for free at:

<http://advances.sciencemag.org/content/2/4/e1501801#BIBL>

Science Advances (ISSN 2375-2548) publishes new articles weekly. The journal is published by the American Association for the Advancement of Science (AAAS), 1200 New York Avenue NW, Washington, DC 20005. Copyright is held by the Authors unless stated otherwise. AAAS is the exclusive licensee. The title *Science Advances* is a registered trademark of AAAS